Three-Dimensional Models of Estrogen Receptor Ligand Binding Domain Complexes, Based on Related Crystal Structures and Mutational and Structure−Activity Relationship Data†

Jean-Marie Wurtz,‡ Ursula Egner,§ Nikolaus Heinrich,§ Dino Moras,‡ and Anke Mueller-Fahrnow*,§

Laboratoire de Biologie Structurale, IGBMC, 1, rue Laurent Fries, BP 163, 67404 Illkirch, France, and Research Laboratories of Schering AG, D-13342 Berlin, Germany

Received June 19, 1997

On the basis of the recently determined crystal structures of the ligand binding domains (LBDs) of the retinoic acid nuclear receptors (NRs), we present a three-dimensional (3D) molecular model of the human estrogen receptor alpha (hERα) LBD. A literature search for mutants affecting the binding properties has been performed; 45 out of 48 published mutants can be explained satisfactorily on the basis of the model. Estradiol has been docked into the binding pocket to probe its interactions with the protein. Energy minimizations and molecular dynamics calculations were performed for various ligand orientations. To evaluate their quality, the different models were scored using known structure−activity relationship (SAR) data for selected close estradiol homologues. The two best models explain largely the binding affinities of more distantly related ligands.

Introduction

The estrogen receptor (ER) plays a crucial role in many processes such as the control of reproduction and the development of secondary sexual characteristics.[1−4] The ER belongs to the superfamily of nuclear receptors (NRs), including the steroid, thyroid (TR), and retinoic (X, RXR; acid, RAR) receptors. These ligand-activated transcription factors modulate the expression of specific genes.[5−8] All NRs consist of five to six domains, the most conserved among them are the DNA binding domain (DBD) and the ligand binding domain (LBD).[7]

Up to now, three-dimensional (3D) structures have only been determined for isolated domains, for DBDs,[9−16] and, more recently, for LBDs. The published X-ray structures (see Addendum) are that of the apoform of the human RXR alpha (hRXRα),[17] the human RAR gamma (hRARγ) in a complex with *all-trans*-retinoic acid (TRA),[18] and the rat TR alpha (rTRα1) liganded with a thyroid hormone agonist.[19] A sequence/structure comparison provided evidence that NR LBDs share a conserved architecture revealing a novel fold.[20] The crystal structures provide a good starting point for modeling that had not been available for earlier studies.[21,22] Homology-derived models have been proposed for the RAR and RXR LBDs bound to different ligands as well as for the glucocorticoid receptor (GR) LBD bound to dexamethasone, a synthetic agonist.[20]

We present a 3D model of the human ERα (hERα) LBD bound to estradiol (E2) based on the crystal structure of the hRARγ/TRA. To put the model on a more solid basis, we have analyzed the impact of numerous published natural and engineered mutations. The binding affinities of several E2 derivatives were examined to probe the ligand position in the ligand binding pocket (LBP).

Results and Discussion

Sequence Alignment. In the sequence alignment of NR LBDs, the N- and C-termini of the helices, derived from the hRXRα and hRARγ LBD crystal structures, were used as anchoring points[20] (Figures 1 and 2). Only the liganded hRARγ, which has a sequence identity of 21% with hERα LBD, is used in the modeling work described below; the hRXRα has only been included for comparison purposes (Figure 1). Besides the insertions and deletion discussed in Model Building, the most variable regions are the loops connecting the helices, in particular loop 1−3, loop 6−7, and loop 8−9. Most of the conserved residues belong to the NR signature (region H3−H5)[20] or to helices H10−H12. The hERα numbering is used throughout the text if not otherwise mentioned, even when mouse ER (mER) mutants are discussed.

Model Building. On the basis of the assumption that NR LBDs share a conserved 3D architecture,[20] the 11 helices in hRAR have been taken as a template for the hERα LBD model. According to the sequence alignment (Figure 1), which is the basis of our models, three insertions (1 amino acid in loop 6−7, 8 amino acids in loop 8−9, 3 amino acids in loop 9−10) and one deletion (10 amino acids in loop 1−3) have been identified in hERα LBD (Figures 1 and 2, top). Loop 1−3 is in the vicinity of the LBP; therefore an indirect influence on the size and shape of the cavity seems likely. A loop conformation proposed by MODELER[23](see Methods) for this area was modified to resemble that of hRAR.

† Abbreviations: 3D, three-dimensional; GR, glucocorticoid receptor; DBD, DNA binding domain; E2, estradiol; ER, estrogen receptor (hERα, human ERα); RAR, retinoic acid receptor (hRARγ, human RARγ); RXR, retinoic X receptor (hRXRα, human RXRα); LBD, ligand binding domain; LBP, ligand binding pocket; NR, nuclear receptor; RBA, relative binding affinities (%) to ER (rat uterus, incubation time 2 h, 4 °C), if not otherwise stated, E2 ≡ 100%; rmsd, root-mean-square deviation; SAR, structure−activity relationship; rTRα, rat thyroid hormone receptor α; TRA, *all-trans*-retinoic acid.

* Corresponding author. Tel: +49-30-4681 7699. Fax: +49-30-4681 6741. E-mail: anke.muellerfahrnow@schering.de.

‡ IGBMC.

§ Research Laboratories of Schering AG.

S0022-2623(97)00406-8 CCC: $15.00
Published on Web 05/01/1998

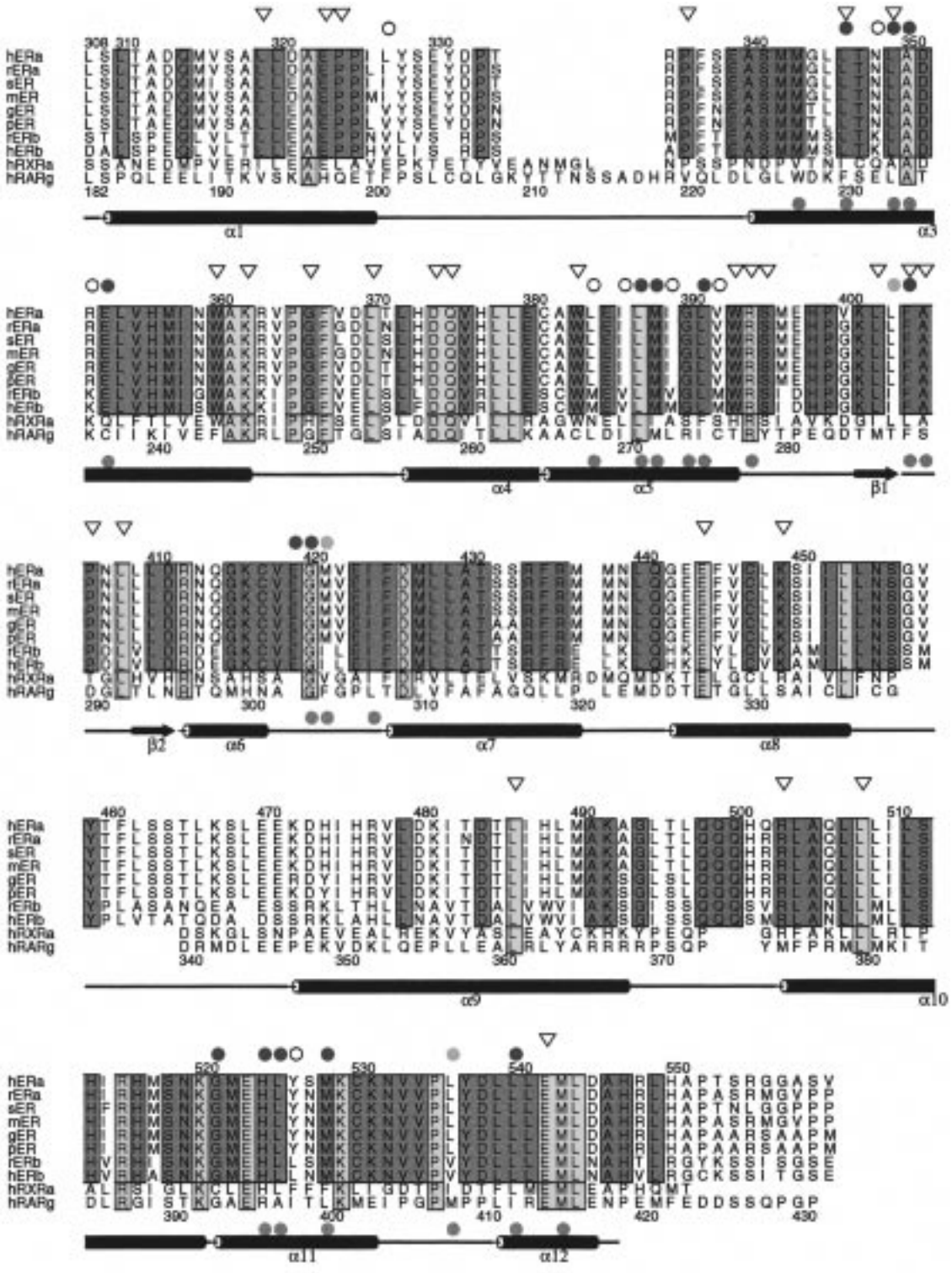

Figure 1. Sequence alignment of estrogen nuclear receptor ligand binding domains (LBDs). The alignment includes estrogen receptors from numerous organisms and also the human and rat α- and *β*-isoforms. The sequences of the hRXRα and hRAR*γ* for which crystal structures have been determined are also included. The organism abbreviation and accession numbers are: h, *Homo sapiens* (M12674 and X99101 for α- and *β*-isoforms); r, *Rattus norvegicus* (X61098 and U57439 for α- and *β*-isoforms); s, *Sus scrofa* (Z37167); m, *Mus musculus* (M38651); g, *Gallus gallus* (X03805); p, *Poephila guttata* (L79911). The alignment has been derived as described in the Methods section. The sequence numbering above and below the alignment is for the hERα and the hRAR*γ*, respectively. Identical residues in the whole alignment are highlighted in yellow. Blue-shaded boxes indicate the identical residues in the ER family; triangles above the sequences indicate residues conserved throughout the steroid receptor family. The secondary structure information shown below the alignment corresponds to the hRAR*γ* crystal structure.[18] The residues closer than 4.5 Å to the ligands are indicated by green or blue dots for the hERα/E2 model and the hRAR*γ*/TRA complexes, respectively. Red and open dots mark residues differing between hERα and hER*β* within 6 and 8 Å of the ligand. The figure was prepared using ALSCRIPT.[58]

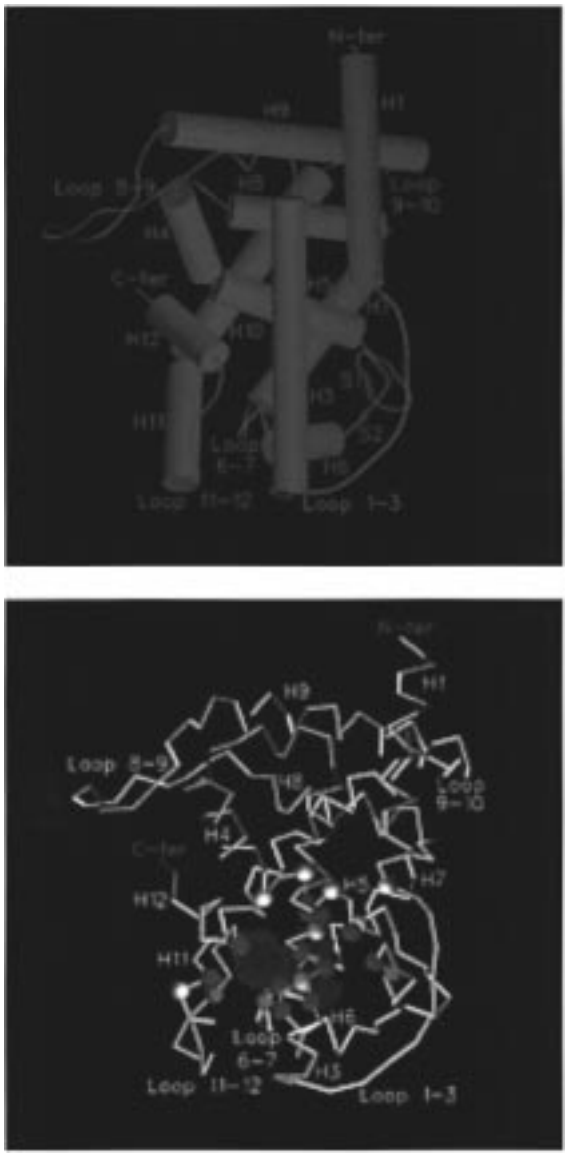

Figure 2. Presentation of the hERα model. (Top) Cartoon showing the overall fold of the hERα LBD with α-helices drawn as cylinders and β-strands as arrows. Insertions and deletions with respect to the hRARγ are colored red and blue, respectively. (Bottom) Cα-Trace of the hERα model. The putative ligand binding cavity is depicted as a blue chicken wire surface. Residues in close vicinity (4.5 Å) of the ligand are conserved between the two isoforms; they are indicated by green spheres. Residues within a shell of 6 and 8 Å around the ligand that differ between the ER α- and β-isoforms are represented as red (3) and white (7) spheres, respectively. The figures were produced with SETOR.[59]

The one-amino acid insertion (Glu419) in loop 6−7 is unique among NRs but conserved in the ER family. Its position close to the putative LBP strongly suggests a special role of this residue in polar ligand binding contacts. One way to accommodate the insertion is to extend helix H6. With this strategy, Glu419 points away from an significantly enlarged LBP that is inconsistent with the size of E2 (TRA and E2 volumes are 278 and 233 Å^3 as calculated with GRASP,[24] respectively). In the second approach, different loop geometries have been generated[25] taking the C- and N-termini of helices H6 and H7 as anchoring points. From five thus obtained models, a clear favorite was identified with Glu419 pointing into the LBD, the size of which is in agreement with the volume of E2. The conformation of loops 8−9 and 9−10 were accepted as proposed by MODELER.[23] The presumably flexible loop 8−9 could come in close contact to the amphipatic α-helix H12, important for all transcriptionally active NRs.[7,20] Unfortunately, this loop is too long to be reliably predicted without additional structural information from homologous proteins. The loop 9−10 is located far away from the ligand binding niche, and its conformation should have no effect on ligand binding.

Analysis of Mutant Data. Because of the low homology between the hRAR and hERα LBDs (21% sequence identity over a 237-residue range; Figure 1) special care was taken with the evaluation of the hERα LBD model. We carried out a literature search (from 1989 to 1996, see Table 1 and references therein) to retrieve mutants affecting the binding properties of the human or mouse ER which exhibit 96% sequence identity for the LBDs (Figure 1). Since some of the mutants were published with varying binding affinities by different authors, we decided to group the mutants in the following way: 12 mutants reducing the binding affinity by at least a factor of 10 were considered to have a pronounced impact (Table 1a), 14 mutants affecting the binding affinity by a factor of 2−10 were considered to have a moderate influence (Table 1b), and 22 mutants reducing the binding affinity by less than a factor of 2 were considered to have no influence (Table 1c).

Selected examples for mutants including some that had not been found with the literature search are the following:

(1) The E2 binding affinity for the H524A mutant is more than 10-fold reduced as compared to the wild-type protein.[26] This loss of affinity is in agreement with our models as we have postulated a hydrogen bond between His524 and a hydroxyl function of E2 (see Estradiol Docking and Figure 3).

(2) E2 binds only weakly to the G525R mutant of mER[27,28] (G521R of hERα, helix 10), and only 10−35% of the wild-type activity as well as reduced binding affinity are observed for the G521A mutant.[26] In the model, Gly521 is only one helical turn apart from His524 which is assumed to be hydrogen-bonded to the ligand (see above). The effect of the mutation can easily be explained by an unfavorable steric contact or by the introduction of a charge in close proximity to the ligand.

(3) The L525A mutant has less than 10% of the wild-type activity, and the specific binding is too low to obtain an accurate K_d for E2.[29] In our models, Leu525 is in close vicinity to E2. In addition, this residue might be necessary to stabilize the positions of His524 (see above) and helix H12, as close interactions are observed in our models with residues Leu544 and L536 (both H12). This last assumption is supported by the instability of the mutant in the absence of hormone.[26]

Only 3 out of 48 mutants published during the last 7 years could not be explained satisfactorily on the basis of our model: L539A,L540D,[30] M543A,L544D,[30] and D538V.[31] The E2 binding affinities of the two double mutants L543A,L544D[30] and M547A,L548D[30] of mER (L539A,L540D and M543A,L544D of hERα, respectively) are lowered by a factor of 2−3 as compared to the wild-type protein. Leu540 and Leu544 are located on helix H12 and are predicted to be in the vicinity of

Table 1. Mutants of the ER Reducing the Ligand Binding Affinity of the Given Ligand[a]

a. By a Factor of 10 or More

mouse	human	position	
	V364E estradiol[31]	loop 3−4	√
	W383R estradiol[31]	H5	√
	D426Y estradiol[31]	H7	√
	C447Y estradiol[31]	H8	√
	R503L estradiol[31]	H10	√
L511D, I518D iodoestradiol[27]	L507D, I514D	H10	√
I514V, I518R iodoestradiol[27]	I510V, I514R	H10	√
I518R iodoestradiol[27] estradiol[28]	I514R	H10	√
	K520D, G521R, E523R, H524L estradiol[45]	H10, H11	√
G525R iodoestradiol[27] estradiol[28]	G521R	H11	√
G525D, M532D iodoestradiol[27]	G521D, M528D	H11	√
	D538V estradiol[31]	H12	

b. By a Factor of 2−10

mouse	human	position	
	D351V, R548L estradiol[31]	H3, F-domain	(√)[b]
	C381A, C417A, C447A, C530A estradiol[46]	H4, H6, H8, H11	√
	G400V estradiol[47]	loop 5−β1	√
	E523Q estradiol[32]	H11	
L529A, M532A, C534A,V537A estradiol[28]	L525A, M528A, C530A, V533A	H11, loop 11−12	√
M532R estradiol[28]	M528R	H11	√
	K529Q, K531Q estradiol[32] OH-tamoxifen[32]	H11	√
	K529Q, K531Q, N532D estradiol[32] OH-tamoxifen[32]	H11	√
L543A, L544A estradiol[30]	L539A, L540A	loop 11−12, H12	√
L543A, L544D estradiol[30]	L539A, L540D	loop 11−12, H12	
	L540Q estradiol[31,48−50] OH-tamoxifen[31,50]	H12	
M547A, L548A estradiol[30,51]	M543A, L544A	H12	√
M547A, L548D estradiol[30]	M543A, L544D	H12	
D549A estradiol[30]	D545A	H12	√
	D374N, E380Q, E385Q estradiol[52]	H4, H5	√
	E380Q estradiol[52]	H4	√
	C381A estradiol[53]	H4	√
	C381A, C530A estradiol[46]	H4, H11	√
	K416Q estradiol[52,53]	H6	√
	C417A estradiol[53]	H6	√
	C417A, C530A estradiol[46]	H6, H11	√

Table 1 (continued)

c. By Less Than a Factor of 2

mouse	human	position	
	C447A estradiol[53]	H8	√
	C447A, C530A estradiol[46]	H8, H11	√
	K449Q estradiol[52]	H8	√
R507A iodoestradiol[27]	R503A	H10	√
L511R iodoestradiol[27]	L507R	H10	√
	E523Q, D538N estradiol[32]	H11, H12	√
	C530A (or S) estradiol[53]	H11	√
	N532D estradiol[32]	H11	√
D542A estradiol[30]	D538A	H12	√
	D538N estradiol[32]	H12	√
D542A, E546A, D549A estradiol[30]	D538A, E542A, D545A	H12	√
D542N, E546Q, D549N estradiol[51]	D538N, E542Q, D545N	H12	√
	L540Q, E542A, D545A estradiol[50]	H12	√
E546A estradiol[30]	E542A	H12	√
	E542A, D545A estradiol[50]	H12	√

[a] For experiments carried out with the mER, the corresponding residues of the hER are also given. Mutants for residues involved in ligand binding are underlined. A "√" in the last column is indicative of an altered binding affinity that can be explained on the basis of the model. [b] As no structural data are available for the region encompassing R548, this mutation cannot presently be analyzed. However, the observed binding behavior of the double mutant is in agreement with the expected effect of the D351V mutation.

the ligand. We therefore expected the substitution of the apolar side chains by charged ones to have a more pronounced effect on E2 binding affinity. Asp538, a conserved residue in the loop 11−12, is located on the protein surface. The 20-fold decrease in the E2 binding affinity for the D538V[31] mutant is especially difficult to understand since neither D538A[31] nor D538N[32] exhibit an impaired binding behavior.

Estradiol Docking. The hERα ligand binding cavity is lined by highly hydrophobic residues (Figure 1; green spheres in Figure 2, bottom). The only potential interaction sites for the steroidal hydroxyl groups at positions 3 and 17 identified with the GRIN and GRID programs[33] are located at opposite positions in the cavity: Glu353 (helix H3) stabilized by a salt bridge to Arg394 (helix H5) and His524 (helix H11) together with Glu419 (loop 6−7). In addition, Glu419 can be postulated to participate in a hydrogen bond network involving Lys531 and Asn532 (Figure 3). The existence of such a hydrogen bond network is supported by mutagenesis data:[32] substitution of Lys531 or Asn532 leads to an impaired ligand binding affinity although no direct contacts are observed with the ligand.[32] All above-mentioned residues are strongly conserved in the ER family.

On the basis of the model alone, it cannot be decided which E2 hydroxyl group is oriented toward helices H3 and H11. The ligand is said to be in the A or D orientation, if the A- or D-ring is oriented toward helix H11 (Figure 3), respectively. From SAR data for different organisms it is well-established that the two hydroxyl groups of E2 contribute differently to the binding affinity.[34] The removal of 17β-OH reduces the

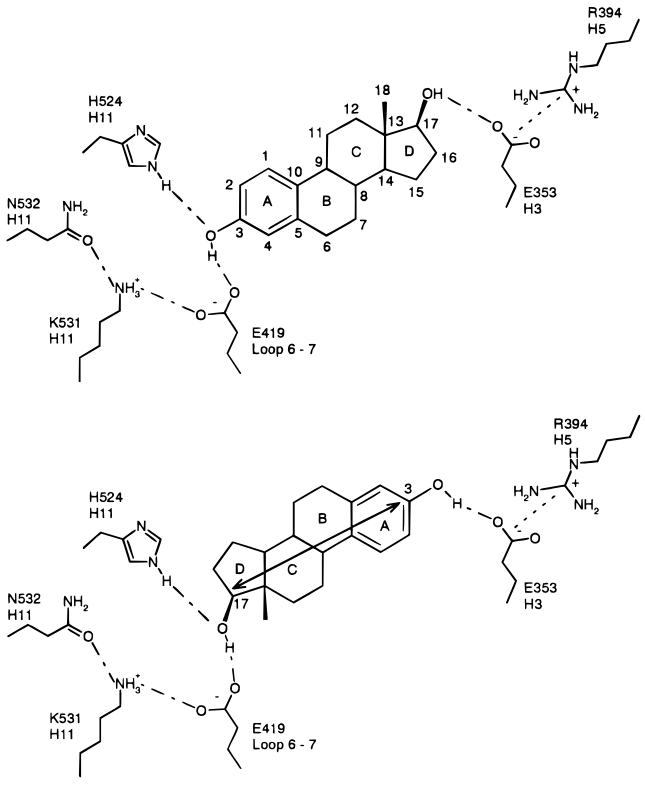

Figure 3. Schematic presentation of the main polar interactions involved in ligand binding in the A and D models. The numbering scheme for estradiol is shown. The rotation axis mentioned in the text is indicated.

Table 2. SAR of Estradiol Analogues[54] Used for Scoring (See Text)[a]

	RBAs (%) for E2 derivatives			
position	-OH	$-CH_3$	others	remarks
1	6.9	20.4	$-CH_2OH$: 5.0	small hydrophobic substituents are tolerated
2	8.3	11.1	$-OCH_3$: <0.2	introduction of smaller hydrophobic substituents is possible
4	16.4; 40.0[55]	25.0	-C≡N: 1.4	small substituents are tolerated
6α	<0.4			only small hydrophobic substituents may be tolerated
6β			6β-ethynyl E2: 310, 6β,7β-methylene E2: 97	even for small substituents a steric hindrance is expected
7α	<1	83.3		introduction of a small hydrophobic substituent is possible, hydrophilic substituents are not tolerated
7β		~10		even for smaller groups steric hindrance is expected
14α	6.7	31.3	$-C_2H_5$: 33.3	small hydrophobic substituents are tolerated, hydrophilic groups are less suited
15α	2.5	143	$-CH_2$Phe: 55	small hydrophobic substituents increase the binding affinity, hydrophilic groups are not tolerated
15β		37		small hydrophobic substituents are tolerated
16α	13.5	67.2[56]		small hydrophobic substituents are better tolerated than hydrophilic ones
16β			$-C_2H_5$: 5.1	even small substituents cause steric problems
17α			-C≡CH: 200	
12β	3.0			hydroxy substituent (unitary) is not tolerated
11β	9.1	125[57]	-*p*-hydroxyphenyl: 40	introduction of hydrophobic groups of different sizes is possible

[a] If no RBAs are available for the respective methyl or hydroxy derivatives of estradiol, data for related compounds have been used to derive the statements given as remarks. The positions 3 and 17β of the steroid were not considered in the scoring as restraints were applied to stabilize the polar interactions during the calculations.

binding affinity toward rERα by a factor of 44 (relative binding affinity, RBA = 1.9%[35]). An even weaker binding is observed in the absence of 3-OH. This could indicate that the 3-OH group is involved in a stronger hydrogen-bonding environment than 17β-OH and should be oriented toward His524 and Glu419, corresponding to an A orientation. On the other hand, in the hRARγ/TRA[18] complex, the TRA carboxylate group (critical for TRA binding, see Comparison with the hRARγ LBP) is oriented toward helix H3, and by analogy the D orientations seem more plausible. Further arguments for the D orientations are:

(1) The hydrogen bond acceptor Glu353 in ER is replaced by Gln in steroid NRs which could serve as either a donor or an acceptor.[20] E2 binds weakly to the other steroid receptors, whereas the other natural 3-keto-Δ^4-ligands do not bind to ER. Therefore, an interaction might be assumed between 3-OH and Glu353.

(2) Photolabeling experiments for GR imply that the D orientations are more plausible.[36]

(3) A favorable $\pi-\pi$ interaction of the aromatic A-ring can be postulated with Phe404 only in the D models. However, Phe404 is conserved throughout the steroid receptor family although E2 is the only natural ligand with an aromatic A-ring.

As no conclusive argument can be found for either the A or D models, both possibilities were further investigated. To retain the primary interactions with the steroidal hydroxy functions (Figure 3), distance restraints were introduced for the calculations described below (see Methods). In addition to the ambiguity concerning the position of the steroidal A- and D-rings, the rather planar E2[37] can be rotated in the pocket around an axis defined by C3 and C17. A total of eight orientations have been considered by rotating the steroid skeleton in steps of 90° around the C3/C17 axis for the A and D orientations. The respective models are referred to as A0, A90, A180, A270, and D0, D90, D180, D270. In the A0 and D0 models, C18 of E2 points toward helix H6. For the eight different E2 orientations described above, energy minimizations and molecular dynamics calculations were performed in the presence and absence of a 10 Å water layer using the protocols described in the Methods section. Thus, 32 different model structures were obtained.

Analysis and Scoring of the Models. The stability of the α-helices was employed as a criterion to test the suitability of the models. All molecular dynamics simulations and the energy minimizations in the absence of water resulted in severely distorted structures which were discarded. In contrast to these results, energy minimizations performed with a 10 Å layer of water molecules led to reasonably stable secondary structures, and only these models were subjected to further evaluation. Superpositions of the minimized models with the initial structure resulted in rmsd values of 0.7−1.2 Å for all equivalent Cα-atoms.

During the geometry optimizations, the positions and orientations of the bound ligand molecules were modified significantly with respect to their starting orientations. In the A models, E2 was initially located farther away from helices H11 and H12 than in the D models, but shifts in the course of the minimization brought the ligands into comparable positions. In both the A and D models, the steroid planes were rotated up to 110° around the C3/C17 axis (Figure 3). The E2 positions therefore almost coincide in two of the refined A and D models (former A0/A90 and D0/D90, respectively). The results of the calculations indicate a preference for the plane occupied by the ligands in these four refined models. Furthermore, in an additional D model the steroid skeleton is found in the same plane but rotated by approximately 180° around the C3/C17 axis.

The final criterion for the scoring of the remaining eight models exploited known SAR for selected close E2 homologues with the binding behavior predicted on the basis of the respective model structures. To avoid ambiguities concerning the binding mode which could be caused by large substituents, we preferentially used the methyl and hydroxy derivatives. These substituents are approximately of the same size and allow to probe the steric demand or the hydrophobic/hydrophilic nature

Table 3. Scoring of the Estradiol Orientations in the 3D Models Based on a Comparison with SAR Data for Selected Agonists (See Text)[a]

starting models	+	?	−	score[b]	final models
A0	10	3	2	11.5	A*
A90	7	6	2	10	
A180	2	8	5	6	
A270	4	3	8	5.5	
D0	7	6	2	10	
D90	8	6	1	11	D*
D180	4	6	5	7	
D270	5	4	6	7	

[a] The best models are A0 and D90; they have the highest scores. After energy minimization, A0/A90 and D0/D90, respectively, converged to very similar structures, and the best in each group is designated as models A* and D* (see text). [b] To obtain a numerical score, the following definitions have been made: + = 1.0, ? = 0.5, and − = 0.0; example, A0: (1.0×10) + (0.5×3) + (0.0×2) = 11.5.

at a given position. In addition, general remarks were deduced from other SAR data (Table 2). This information was combined to rate each of the 15 positions of the steroid listed in Table 2 for the eight models (see Methods). The ratings for the individual positions were then combined to give the global scores of the models as shown in Table 3. The minimized forms of models A0, A90, D0, and D90 are the best ones having the highest scores (10.0−11.5); in each of these models, disagreement with known SAR was encountered for only one or two positions of the steroid. The remaining models are significantly inferior to the others. As already pointed out, the positions of the ligands in the refined models A0/A90 and D0/D90, respectively, are very similar. We therefore decided to use only the best A and D models (Figure 4, top, middle) for the subsequent analysis and docking of other ligands and called them models A* and D*, respectively. Note that the 3-OH hydrogen bond in the D* model is in plane with the aromatic A-ring, whereas in the A* model a deviation from planarity is observed.

PROCHECK[38] confirmed that the geometry and the dihedral angles of these structures were in a range expected for a good protein structure;[39] e.g., in all models, more than 98% of the residues are in the most favorable or allowed regions of the Ramachandran plot. In model A*, four residues are in generously allowed regions (Arg335 and Pro336 in loop 1−3, Asn 407 in loop β1−β2, Glu419 in loop 6−7) and only Asp332 (loop 1−3) is in a disallowed region. Unfavorable geometries are observed for the same residues in model D*.

Ligand Binding Pocket. As the calculations included water molecules, we analyzed the distribution of solvent molecules around the LBP. In model A*, only one water molecule was observed in the vicinity of the ligand. It is located below the center of the steroidal A-ring (in the standard orientation of steroids) and is hydrogen-bonded to Gly521(O). The role of this water is not clear. Note that its presence does not lead to a significant increase in the size of the LBP at this position as compared to the hRARγ structure. In model D*, three water molecules are accommodated within the LBP and a few more in its vicinity. As in model A*, one water molecule is hydrogen-bonded to Gly521(O); it is less than 5 Å away from positions C11, C12, and C18 of the steroid. The other water molecules extend the hydrogen bond network around O3. One of them provides an additional bridge between O3 and Glu353, whereas the others connect Glu353 with the protein surface via a chain of hydrogen bonds.

Residues in contact with the ligand (heavy atom distances closer than 3.8 Å) are Leu346 (only A*), Ala350, Glu353, Leu354 (only D*), Leu387, Leu391, Phe404, Glu419, Gly420 (only A*), His524, Leu525 (only A*), and Leu540 (only A*); they are strictly conserved in the ER family (Figures 1 and 2, bottom). Interestingly, the ER α- and β-isoforms, which have approximately 60% sequence identity, differ at three positions (Leu403/β1, M421/loop 6−7, L536/loop 11−12) in a shell of 6 Å around the ligand. Eight additional variable residues are identified in a shell up to 8 Å (Leu327/H1, Asn348/H3, Arg352/H3, Leu384/H5, Ile386/H5, Ile389/H5, Val392/H5, Y526/H11; Figures 1 and 2, top). Note that most of the variable residues are located in helix H5 (Figure 2). These differences could result in a modified binding behavior toward some bulkier ligands in hERβ as compared to hERα.

Comparison with the hRARγ LBP. As the structurally conserved regions have been tethered during the energy minimizations, differences between hRARγ and hERα are found mainly in loop regions (see Model Building and Methods). The Cα-trace superposition of the hRARα and hERα LBDs exhibits a rmsd of 0.7 and 1.1 Å in the A* and D* models, respectively. E2 is almost in plane with TRA in model A*, whereas in model D* the ligand is slightly shifted (Figure 4, bottom). A comparison of the highly hydrophobic binding cavities of the hRARγ and hERα structures reveals a smaller pocket for the latter consistent with the smaller size of E2. Ala397 in hRARγ that delimits the length of the LBP is replaced by Leu525 in hERα. The importance of Leu525 for E2 binding has been shown recently.[26,29] Among the residues lining the hERα LBP (heavy atom distances to the ligand less than 4.5 Å), six identities with hRARγ are observed: Leu349/233, Ala350/234, Leu387/271, Met388/272, Phe404/288, and G420/303, in hERα and hRARγ, respectively. The polar residue Arg394 (Arg278 in hRARγ, highly conserved in NRs[20]), at the C-terminus of helix H5, is 5 Å apart from the ligand and engaged in a salt bridge with Glu353. In hRARγ, this arginine anchors the TRA carboxylate group. In our model, Glu353, replacing a cysteine in hRARγ, plays the role of the TRA carboxylate to contact the arginine (Figure 4, bottom left) and also forms a critical hydrogen bond with one of the steroidal hydroxyl groups at position 3 or 17 in the D* or A* orientation, respectively.

Docking of Other Ligands. No preference for model A* or D* can be deduced from the analysis of close E2 homologues as both models are largely in agreement with the experimental SAR data. The same ambiguity was also encountered by other groups (e.g., see refs 26 and 29). Therefore, both A* and D* models were used to dock the more distantly related ligands **1**−**10** (Table 4) which were selected to investigate special aspects of ligand binding and to further evaluate the usefulness of the models.

The D-homo derivatives **1**−**3** were chosen to analyze the influence of a modified steroid skeleton.

The inversion of the stereochemistry at C17 of E2 (compound **4**) has a pronounced effect on the binding

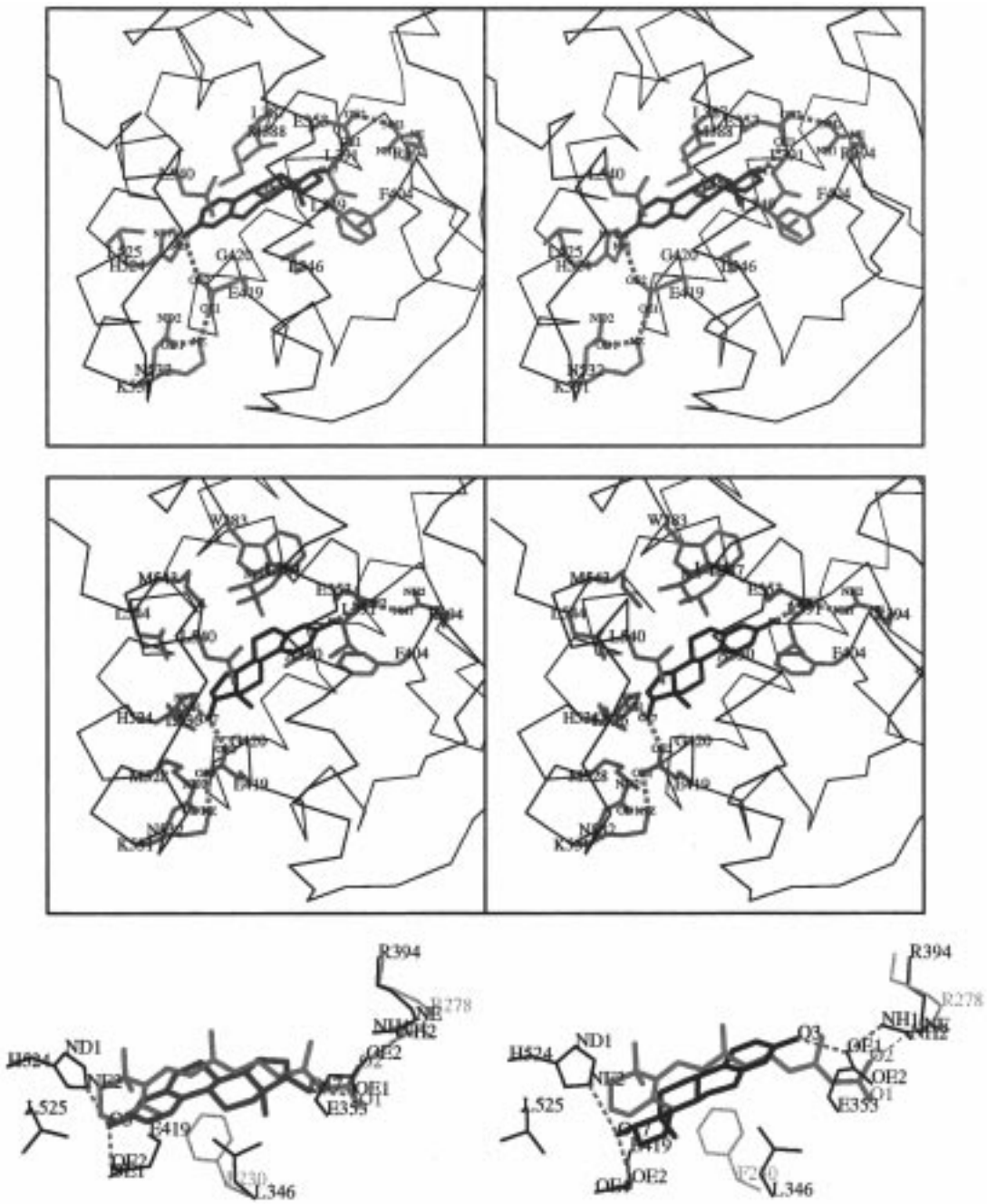

Figure 4. Position of estradiol in the ligand binding pocket of the hERα (top) A* and (middle) D* models. Part of the receptor backbone is drawn as Cα-trace; side chains are only shown for residues closer than 4.5 Å to the ligand. The hydrogen bond network discussed in the text is depicted as red dashed lines. The ligand orientation in the (bottom left) A* or (bottom right) D* model is compared to the position of the *all-trans*-retinoic acid (magenta) as seen in the crystal complex. Black- or gray-colored side chains of key residues belonging to the hERα or hRARγ receptor, respectively, are included. In all representations, estradiol is drawn in green or blue in the A* or D* orientation, respectively. The figures were produced with MOLSCRIPT.[60]

affinity that is not observed for the 14,16α-ethano-bridged compounds **5** and **6** having different D-ring conformations. A superposition of the steroid skeletons of E2 and compounds **4**−**6** results in the 17-OH orientations shown in Figure 5, which might be the reason for the different binding behaviors.

Nonadditive substituent effects can be illustrated with compounds **7** and **8**. Methylation of the aromatic 2-position (compound **7**) leads to a 6.5-fold reduction of the binding affinity, and the 16-ethyl derivative (compound **8**) binds about 20 times weaker to hERα than E2. The 2,16-dimethyl derivative **9** (RBA < 0.2), however, deviates by a factor of at least 4 from what one might expect from a simple additivity scheme of substituent effects.

The anordrin derivative **10** is of special interest because it lacks the aromatic A-ring commonly anticipated to be essential to high-affinity ER ligands and because of its two rigid ethynyl substituents.

Can the RBA differences observed within each set of compounds be explained by the A* and/or D* model? In Table 4, the expected binding behavior deduced from the models is compared to the experimental RBAs. The modification of the D-ring in compounds **1**−**3** has no influence on the hydrogen bonds in both models. However, bad steric contacts led us to predict a lower binding

Table 4. RBAs for Selected ER Ligands (Compounds **1**−**10**)[a]

Compound	A*	D*
1 (RBA = 27.8) 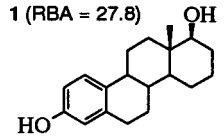	Similar hbond ✓ steric ✓	Similar hbond ✓ steric ✓
2 (RBA = 11.2) 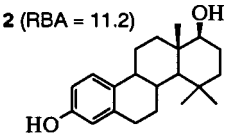	Lower hbond ✓ steric −	Lower hbond ✓ steric −
3 (RBA = 1.1) 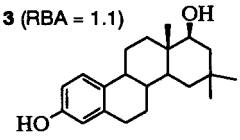	Similar hbond ✓ steric −	Higher hbond ✓ steric ✓
4 (RBA = 2.2) 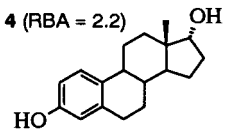	Similar hbond − steric ✓	Similar hbond − steric ✓
5 (RBA = 111.1) 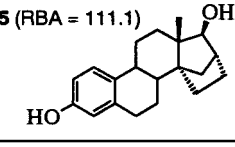	Lower hbond ✓ steric ✓	Lower hbond − steric ✓
6 (RBA = 125) 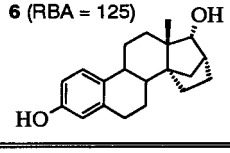	Similar hbond ✓ steric ✓	Similar hbond ✓ steric ✓
7 (RBA = 15.4) 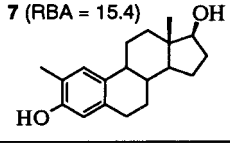	Higher hbond ✓ steric ✓	Similar hbond ✓ steric −
8 (RBA = 5.1) 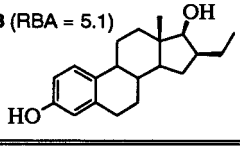	Similar hbond ✓ steric −	Higher hbond ✓ steric ✓
9 (RBA < 0.2) 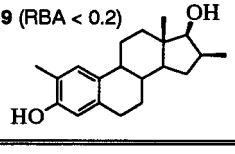	Similar hbond ✓ steric −	Similar hbond ✓ steric −
10 (RBA = 13.3) 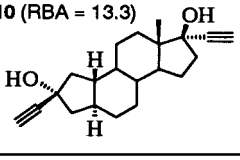	Similar hbond − steric ✓	Similar hbond − steric ✓

[a] For each compound the predicted binding affinity, relative to the experimental RBA, is indicated (lower, similar, higher). Favorable polar (keyword: hbond) or van der Waals (keyword: steric) interactions are indicated by a √, whereas − is indicative of an unfavorable situtation.

affinity for compound **2** (RBA = 11.2). The effect of the 17-inversion is at least partially in agreement with the two models: the low binding affinity of 17α-OH E2 is reflected in the loss of one hydrogen bond which is maintained in the bridged compound **6** (RBA = 125) because of the altered 17-OH orientations (Figure 5). However, it cannot be understood why compound **5** has a higher binding affinity than E2; in model D*, the additional steric demand of the ethano bridge even leads to the loss of one hydrogen bond. Both models have problems to explain one of the two monosubstituted compounds **7** and **8**, whereas the low binding affinity of compound **9** had been predicted correctly because of unfavorable steric contacts. The situation with the anordrin derivative **10** is more complicated. In both models, docking of the compound results in the loss of one hydrogen bond to 17β-OH which is predicted to be retained if the OH group is attached to the 16α position. Note that in model D*, the steroid skeletons of E2 and compound **10** are almost perpendicular to each other. Altogether, a reasonable binding behavior would have been predicted for 7 or 6 out of the 10 ligands using model A* or D*, respectively. Therefore, it is still not possible to identify a preference for either model.

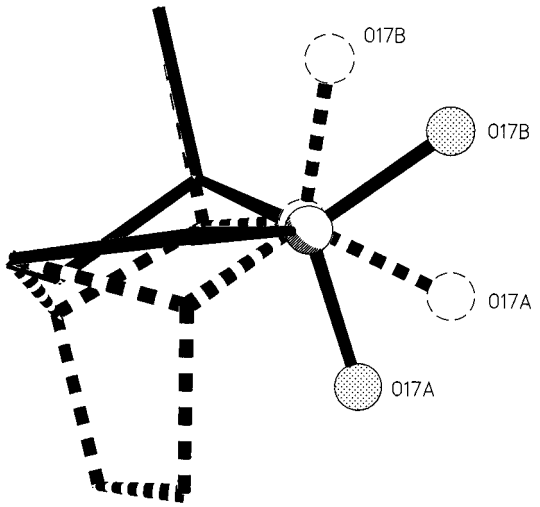

Figure 5. Schematic representation of D-ring only. The 17-OH orientations for E2, 17α-E2 (compound **4**), and the 14,-16α-ethano-bridged compounds **5** and **6** are drawn with dashed lines. The figure was produced with the program XP.[61]

Summary and Outlook

In this contribution, we present the first 3D model of the hERα LBD based on the crystal structure of a homologous protein, the hRARγ LBD. Mutant data from a literature search have been taken into account to validate and improve the model. Its quality with respect to these data is convincing: 45 out of 48 mutations affecting the binding behavior could be explained satisfactorily.

The LBP is lined by long-chain hydrophobic amino acids. The only polar functions located at opposite ends of the cavity, Glu353 (helix H3) and Glu419/His524 (helix H11), respectively, have been identified as putative hydrogen bond partners for the two hydroxyl functions of E2. Both glutamic acids have been modeled to be further involved in polar interactions with Arg394 and Lys531/Asn532, respectively. All these amino acid residues are conserved throughout the ER family. Furthermore, no differences are found between hERα

and hERβ in the immediate environment of the LBP, but 11 residues differ within an 8 Å shell around the cavity. These differences might indicate an altered binding behavior for sterically more demanding ligands.

E2 has been docked into the LBP in various orientations and energy minimizations, in the presence of a 10 Å water layer, have been performed for the complex structures. The refined models have then been scored using SAR data for close E2 derivatives. For two alternative orientations of the bound ligand, almost no contradictions were encountered concerning the experimental findings. However, it is still not possible to decide whether the steroidal A- or D-ring is oriented toward helix H3 or H11, respectively. This question will be answered by the crystal structure of the hERα LBD/E2 complex which will soon be available. Still, the orientation of the ligand might be influenced by substituents favoring other binding modes.

Methods

Sequence Alignment. The sequence alignment shown in Figure 1 has been obtained with the CLUSTALW package;[41] default parameters were applied. The ER members and the hRXRα and hRARγ sequences were aligned separately and then combined as two rigid groups in a profile alignment. Some manual changes were necessary to correctly align the region encompassing helices H6−H7 because of a one-residue insertion, Glu419 in hERα.[20]

Model Building and Evaluation. The modeling was done using a variety of programs: InsightII/Discover,[42] Sybyl,[43] O,[44] WHATIF.[25] The academic version 2.0 of MODELER was used and run with default parameters.[23] E2 was manually adjusted into the binding niche of the LBD of hERα with hydrogen bonds either to Glu419 and His524 or to Glu353. Energetically favorable binding sites for probe groups (methyl group, hydroxyl group, phenyl group) were determined with the program GRIN and GRID,[33] and their positions relative to the chemical groups of E2 were compared.

Models were evaluated using stereochemical criteria (PROCHECK[38]) and by visual inspection. All models were subjected to force field energy minimizations and molecular dynamics simulations (Discover 2.97[42]) using the CFF91 force field. The automatic parameter assignment reproduced sufficiently the bond lengths and angles found in the crystal structure of E2. The calculations were performed using a cutoff radius of 15 Å and a switching function of 2.0 Å with recalculation of the nearest neighbor list for nonbonded interactions every 20 cycles. Energy-minimized models with a maximum derivative of less than 1.0 kcal Å^{-1} were subjected to a molecular dynamics simulation for 100 ps at a temperature of 300 K. At the beginning of the simulation, the C coordinates of structurally conserved regions were tethered with a force constant of 50 kcal Å^{-2}. The models were soaked with a 10 Å water layer (amounting to ca. 3870 water molecules), tethering the outermost 2 Å layer of water molecules with a force constant of 50 kcal Å^{-2}. The angle was forced to the trans conformation in the calculations with a force constant of 50 kcal rad^{-2}. The amino acid residues aspartic acid, glutamic acid, lysine, and arginine were taken in their charged form leading to a total charge of −7.0 for the LBD. In the calculations including water molecules, a dielectric constant of 1.0 was used; for calculations in the gas phase, the dieletric constant was set to 2.0.

A number of refinement protocols were tested in order to maintain the overall structure of the protein and interactions in the LBD of hERα. In the final protocol used, during the first 1400 cycles of energy minimization, the nonbonded interactions were scaled by 0.5 to release possible constraints in the initial model. In case of the A models, distance restraints were applied for the interactions Glu353 (OE1) and H on 17β-OH, Glu353 (CD) and Arg394 (CZ), His524 (HE) and 3-OH, Glu419 (OE2) and H on 3-OH, Glu419 (OE1) and Lys 531 (NZ), and Asn532 and Lys531 (NZ) to reproduce the hydrogen bond network observed in test runs. In the D models, Glu353 interacted with 3-OH, and His524 and Glu419 with 17β-OH of E2. To maintain the overall structure of the LBD, the C atoms of residues 309−326, 340−362, 372−393, 412−417, 422−437, 442−453, 472−493, and 503−520 were tethered to their original positions. To allow more flexibility for the area around Gly420, a special tether option was applied for this region which allows to modify the tethering constants smoothly as a function of the distance from a single atom of interest. At a distance of 3.5 Å of Glu419 C, the force constant was set to 5 kcal Å^{-2} to reach at 10.0 Å a value of 30.0 kcal Å^{-2}. The main-chain torsional angles were forced to −65° and −40°, respectively, for residues Arg412 and 422−437. After scaling of the nonbonded interactions was removed, the energy of the complex was minimized until the maximum derivative was less than 1.0 kcal Å^{-1}. The geometry optimizations of isolated ligand structures fitted into the binding cavity were conducted utilizing the force field implemented in the program Sybyl.[43]

Scoring of the Models. To facilitate the scoring, a list was prepared with selected known SAR for close homologues of E2 (see Table 2). For each position of the steroid, a "+" was assigned if a model was consistent with the experimentally determined SAR and a "−" if not. In case of ambiguities or if side chains had to be reoriented to achieve agreement with the criteria listed in Table 1, a "?" was given. To obtain a numerical score, each "+", "?", and "−" was subsequently converted to 1.0, 0.5, and 0.0, respectively. The highest score indicates the most plausible model.

Acknowledgment. We thank P. Chambon and H. Gronemeyer for helpful and stimulating discussions, and we are grateful to C. Braestrup, E. Eckle, P. Donner, G.-A. Hoyer, and W.-D. Schleuning for supporting the project. We especially want to mention the contribution of J. R. Bull and the Schering chemists and biochemists whose work has been the basis for the SAR data used in this publication. This work was supported by funds from the Centre National de la Recherche Scientifique (including support from IMABIO) and Association pour la Recherche sur le Cancer.

Addendum

After originally submitting our manuscript, crystal structures of the hERα LBD in complex with E2 and with raloxifene have been published.[40] The orientation of E2 corresponds largely to our D* model, but the steroid is rotated by ca. 180° along the C3/C17 axis and the D-ring position is shifted by one helical turn away from loop 6−7. The interaction with Glu419 which we predicted is thus not observed in the experimental structure. The other three polar interaction partners predicted by us are indeed involved in ligand binding: Glu353, Arg394, and His524. However, we predicted an indirect contact between E2 and Arg394 (see Figure 3), whereas a hydrogen bond is observed in the crystal. Furthermore, one water molecule is hydrogen-bonded to O3 of the hormone. A detailed comparison with the experimental structure has to be postponed until the atomic coordinates are released.

References

(1) Ciocca, D. R.; Roig, L. M. Estrogen receptors in human nontarget tissues: biological and clinical implications. *Endocrinol. Rev.* **1995**, *16*, 35−62.
(2) Sluyser, M. Mutations in the estrogen receptor gene. *Hum. Mutat.* **1995**, *6*, 97−103.

(3) Karnik, P. S.; Kulkarni, S.; Liu, X. P.; Budd, G. T.; Bukowski, R. M. Estrogen receptor mutations in tamoxifen-resistant breast cancer. *Cancer Res.* **1994**, *54*, 349−353.
(4) Katzenellenbogen, B. S. Estrogen receptors: bioactivities and interactions with cell signaling pathways. *Biol. Reprod.* **1996**, *54*, 287−293.
(5) Green, S.; Chambon, P. Nuclear receptors enhance our understanding of transcription regulation. *Trends. Genet.* **1988**, *4*, 309−314.
(6) Evans, R. M. The steroid and thyroid hormone receptor superfamily. *Science* **1988**, *240*, 889−895.
(7) Gronemeyer, H.; Laudet, V. Transcription factors 3: nuclear receptors. *Protein Profile* **1995**, *2*, 1173−1308.
(8) Mangelsdorf, D. J.; Thummel, C.; Beato, M.; Herrlich, P.; Schutz, G.; Umesono, K.; Blumberg, B.; Kastner, P.; Mark, M.; Chambon, P.; et al. The nuclear receptor superfamily: the second decade. *Cell* **1995**, *83*, 835−839.
(9) Luisi, B. F.; Xu, W. X.; Otwinowski, Z.; Freedman, L. P.; Yamamoto, K. R.; Sigler, P. B. Crystallographic analysis of the interaction of the glucocorticoid receptor with DNA. *Nature* **1991**, *352*, 497−505.
(10) Schwabe, J. W.; Chapman, L.; Finch, J. T.; Rhodes, D. The crystal structure of the estrogen receptor DNA-binding domain bound to DNA: how receptors discriminate between their response elements. *Cell* **1993**, *75*, 567−578.
(11) Rastinejad, F.; Perlmann, T.; Evans, R. M.; Sigler, P. B. Structural determinants of nuclear receptor assembly on DNA direct repeats. *Nature* **1995**, *375*, 203−211.
(12) Hard, T.; Kellenbach, E.; Boelens, R.; Maler, B. A.; Dahlman, K.; Freedman, L. P.; Carlstedt Duke, J.; Yamamoto, K. R.; Gustafsson, J. A.; Kaptein, R. Solution structure of the glucocorticoid receptor DNA-binding domain. *Science* **1990**, *249*, 157−160.
(13) Baumann, H.; Paulsen, K.; Kovacs, H.; Berglund, H.; Wright, A. P.; Gustafsson, J. A.; Hard, T. Refined solution structure of the glucocorticoid receptor DNA-binding domain. *Biochemistry* **1993**, *32*, 13463−13471.
(14) Eriksson, M. A.; Berglund, H.; Hard, T.; Nilsson, L. A comparison of 15N NMR relaxation measurements with a molecular dynamics simulation: backbone dynamics of the glucocorticoid receptor DNA-binding domain. *Proteins* **1993**, *17*, 375−390.
(15) van Tilborg, M. A.; Bonvin, A. M.; Hard, K.; Davis, A. L.; Maler, B.; Boelens, R.; Yamamoto, K. R.; Kaptein, R. Structure refinement of the glucocorticoid receptor-DNA binding domain from NMR data by relaxation matrix calculations. *J. Mol. Biol.* **1995**, *247*, 689−700.
(16) Lee, M. S.; Kliewer, S. A.; Provencal, J.; Wright, P. E.; Evans, R. M. Structure of the retinoid X receptor alpha DNA binding domain: a helix required for homodimeric DNA binding. *Science* **1993**, *260*, 1117−1121.
(17) Bourguet, W.; Ruff, M.; Chambon, P.; Gronemeyer, H.; Moras, D. Crystal structure of the ligand-binding domain of the human nuclear receptor RXR-alpha. *Nature* **1995**, *375*, 377−382.
(18) Renaud, J. P.; Rochel, N.; Ruff, M.; Vivat, V.; Chambon, P.; Gronemeyer, H.; Moras, D. Crystal structure of the RAR-gamma ligand-binding domain bound to all-trans retinoic acid. *Nature* **1995**, *378*, 681−689.
(19) Wagner, R. L.; Apriletti, J. W.; McGrath, M. E.; West, B. L.; Baxter, J. D.; Fletterick, R. J. A structural role for hormone in the thyroid hormone receptor. *Nature* **1995**, *378*, 690−697.
(20) Wurtz, J. M.; Bourguet, W.; Renaud, J. P.; Vivat, V.; Chambon, P.; Moras, D.; Gronemeyer, H. A canonical structure for the ligand-binding domain of nuclear receptors. *Nature Struct. Biol.* **1996**, *3*, 87−94. (Published erratum appears in *Nature Struct. Biol.* **1996**, *3* (2), 206.
(21) Goldstein, R. A.; Katzenellenbogen, J. A.; Luthey-Schulten, Z. A.; Seielstad, D. A.; Wolynes, P. G. Three-dimensional model for the hormone binding domains of steroid receptors. *Proc. Natl. Acad. Sci. U.S.A.* **1993**, *90*, 9949−9953.
(22) Lewis, D. F.; Parker, M. G.; King, R. J. Molecular modelling of the human estrogen receptor and ligand interactions based on site-directed mutagenesis and amino acid sequence homology. *J. Steroid. Biochem. Mol. Biol.* **1995**, *52*, 55−65.
(23) Sali, A.; Blundell, T. L. Comparative protein modelling by satisfaction of spatial restraints. *J. Mol. Biol.* **1993**, *234*, 779−815.
(24) Nicholls, A.; Sharp, K. A.; Honig, B. Protein folding and association: insights from the interfacial and thermodynamic properties of hydrocarbons. *Proteins* **1991**, *11*, 281−296.
(25) Vriend, G. WHATIF: a molecular modeling and drug design program. *J. Mol. Graph.* **1990**, *8*, 52−6,29.
(26) Ekena, K.; Weis, K. E.; Katzenellenbogen, J. A.; Katzenellenbogen, B. S. Identification of amino acids in the hormone binding domain of the human estrogen receptor important in estrogen binding. *J. Biol. Chem.* **1996**, *271*, 20053−20059.
(27) Fawell, S. E.; Lees, J. A.; White, R.; Parker, M. G. Characterization and colocalization of steroid binding and dimerization activities in the mouse estrogen receptor. *Cell* **1990**, *60*, 953−962.
(28) Danielian, P. S.; White, R.; Hoare, S. A.; Fawell, S. E.; Parker, M. G. Identification of residues in the estrogen receptor that confer differential sensitivity to estrogen and hydroxytamoxifen. *Mol. Endocrinol.* **1993**, *7*, 232−240.
(29) Ekena, K.; Weis, K. E.; Katzenellenbogen, J. A.; Katzenellenbogen, B. S. Different residues of the human estrogen receptor are involved in the recognition of structurally diverse estrogens and antiestrogens. *J. Biol. Chem.* **1997**, *272* (8), 5069−5075.
(30) Danielian, P. S.; White, R.; Lees, J. A.; Parker, M. G. Identification of a conserved region required for hormone dependent transcriptional activation by steroid hormone receptors. *EMBO J.* **1992**, *11*, 1025−1033. (Published erratum appears in *EMBO J.* **1992**, *11* (6), 2366.)
(31) Wrenn, C. K.; Katzenellenbogen, B. S. Structure−function analysis of the hormone binding domain of the human estrogen receptor by region-specific mutagenesis and phenotypic screening in yeast. *J. Biol. Chem.* **1993**, *268*, 24089−24098.
(32) Pakdel, F.; Katzenellenbogen, B. S. Human estrogen receptor mutants with altered estrogen and antiestrogen ligand discrimination. *J. Biol. Chem.* **1992**, *267*, 3429−3437.
(33) Goodford, P. J. A computational procedure for determining energetically favorable binding sites on biologically important macromolecules. *J. Med. Chem.* **1985**, *28*, 849−857.
(34) Anstead, G. M.; Carlson, K. E.; Katzenellenbogen, J. A. The estradiol pharmacophore: ligand structure-estrogen receptor binding affinity relationships and a model for the receptor binding site. *Steroids* **1997**, *62*, 268−303.
(35) Kaspar, P.; Witzel, H. Steroid binding to the cytosolic estrogen receptor from rat uterus. Influence of the orientation of substituents in the 17-position of the 8 beta- and 8 alpha-series. *J. Steroid. Biochem.* **1985**, *23*, 259−265.
(36) Carlstedt-Duke, J.; Stromstedt, P. E.; Persson, B.; Cederlund, E.; Gustafsson, J. A.; Jornvall, H. Identification of hormone-interacting amino acid residues within the steroid-binding domain of the glucocorticoid receptor in relation to other steroid hormone receptors. *J. Biol. Chem.* **1988**, *263*, 6842−6846.
(37) Busetta, B.; Hospital, M. Structure cristalline et moléculaire de l'oestradiol hemihydrate. *Acta Crystallogr. B* **1972**, *B28*, 560−567.
(38) Laskowski, R. A.; MacArthur, M. W.; Moss, D. S.; Thorntorn, J. M. PROCHECK: a program to check the stereochemical quality of proteins structures. *J. Appl. Crystallogr.* **1993**, *26*, 283−291.
(39) Detailed information available upon request.
(40) Brzozowski, A. M.; Pike, A. C. W.; Dauter, Z.; Hubbard, R. E.; Bonn, T.; Engström, O.; Öhman, L.; Green, G. L.; Gustasfsson, J. A.; Carlquist, M. Molecular basis of agonism and antagonism in the oestrogen receptor. *Nature* **1997**, *389*, 753−758.
(41) Thompson, J. D.; Higgins, D. G.; Gibson, T. J. CLUSTALW: improving the sensitivity of progressive multiple sequence alignment through sequence weighting, position-specific gap penalties and weight matrix choice. *Nucleic Acids Res.* **1994**, *22*, 4673−4680.
(42) Insight II/Discover 2.97; MSI Inc., San Diego, CA, 1995.
(43) Sybyl Version 6.3; TRIPOS Inc., Assoc., St. Louis, MD, 1995.
(44) Jones, T. A.; Zou, J. Y.; Cowan, S. W. Kjeldgaard, Improved methods for binding protein models in electron density maps and the location of errors in these models. *Acta Crystallogr. A* **1991**, *47*, 110−119.
(45) Zhuang, Y.; Katzenellenbogen, B. S.; Shapiro, D. J. Estrogen receptor mutants which do not bind 17 beta-estradiol dimerize and bind to the estrogen response element in vivo. *Mol. Endocrinol.* **1995**, *9*, 457−466.
(46) Reese, J. C.; Wooge, C. H.; Katzenellenbogen, B. S. Identification of two cysteines closely positioned in the ligand-binding pocket of the human estrogen receptor: roles in ligand binding and transcriptional activation. *Mol. Endocrinol.* **1992**, *6*, 2160−2166.
(47) Tora, L.; Mullick, A.; Metzger, D.; Ponglikitmongkol, M.; Park, I.; Chambon, P. The cloned human oestrogen receptor contains a mutation which alters its hormone binding properties. *EMBO J.* **1989**, *8*, 1981−1986.
(48) Katzenellenbogen, B. S.; Bhardwaj, B.; Fang, H.; Ince, B. A.; Pakdel, F.; Reese, J. C.; Schodin, D.; Wrenn, C. K. Hormone binding and transcription activation by estrogen receptors: analyses using mammalian and yeast systems. *J. Steroid. Biochem. Mol. Biol.* **1993**, *47*, 39−48.
(49) Ince, B. A.; Zhuang, Y.; Wrenn, C. K.; Shapiro, D. J.; Katzenellenbogen, B. S. Powerful dominant negative mutants of the human estrogen receptor. *J. Biol. Chem.* **1993**, *268*, 14026−14032.

(50) Montano, M. M.; Ekena, K.; Krueger, K. D.; Keller, A. L.; Katzenellenbogen, B. S. Human estrogen receptor ligand activity inversion mutants: receptor that interpret antiestrogens as estrogens and estrogens as antiestrogens and discriminate among different antiestrogens. *Mol. Endocrinol.* **1996**, *10*, 232−242.
(51) Mahfoudi, A.; Roulet, E.; Dauvois, S.; Parker, M. G.; Wahli, W. Specific mutations in the estrogen receptor change the properties of antiestrogens to full agonists. *Proc. Natl. Acad. Sci. U.S.A.* **1995**, *92*, 4206−4210.
(52) Pakdel, F.; Reese, J. C.; Katzenellenbogen, B. S. Identification of charged residues in an N-terminal portion of the hormone-binding domain of the human estrogen receptor important in transcriptional activity of the receptor. *Mol. Endocrinol.* **1993**, *7*, 1408−1417.
(53) Reese, J. C.; Katzenellenbogen, B. S. Mutagenesis of cysteines in the hormone binding domain of the human estrogen receptor. Alterations in binding and transcriptional activation by covalently and reversibly attaching ligands. *J. Biol. Chem.* **1991**, *266*, 10880−10887.
(54) Schering in-house data if not otherwise mentioned.
(55) Schutze, N.; Vollmer, G.; Tiemann, I.; Geiger, M.; Knuppen, R. Catecholestrogens are MCF-7 cell estrogen receptor agonists. *J. Steroid. Biochem. Mol. Biol.* **1993**, *46*, 781−789.
(56) Bohl, M.; Schubert, G.; Koch, M.; Reck, G.; Strecke, J.; Wunderwald, M.; Prousa, R.; Ponsold, K. Quantitative structure−activity relationships of estrogenic steroids substituted at C14, C15. *J. Steroid. Biochem.* **1987**, *26*, 589−597.
(57) Raynaud, J. P.; Ojasoo, T.; Bouton, M. M.; Bignon, E.; Pons, M.; Crastes de Paulet, A. Structure−activity relationships of steroidal estrogens. In *Estrogens in the Environment II*; McLachlan, J. A., Ed.; Elsevier: New York, 1985; pp 24−42.
(58) Barton, G. J. ALSCRIPT: a tool to format multiple sequence alignments. *Protein Eng.* **1993**, *6*, 37−40.
(59) Evans, S. V. SETOR: hardware lighted three-dimensional solid model representations of macromolecules. *J. Mol. Graph.* **1993**, *11*, 134−138.
(60) Kraulis, P. J. MOLSCRIPT: a program to produce both detailed and schematic plots of protein structures. *J. Appl. Crystallogr.* **1991**, *24*, 946−950.
(61) SHELXTL+ Version 5.03; Siemens Analytical X-Ray Instruments Inc., 1995.

JM970406V